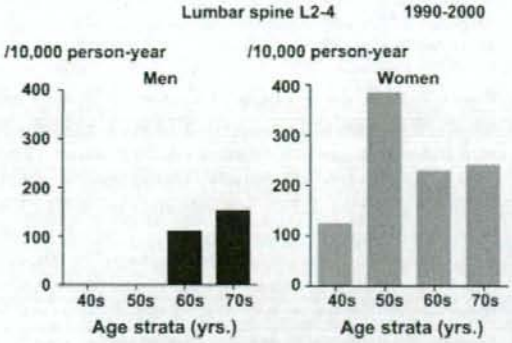

Fig. 2 Incidence of osteoporosis at the lumbar spine over 10 years by age group and gender

Causal relationship between OP and OA

The causal relationships between lumbar OA and OP, BMD, and VFx are summarized in Table 3.

First, the contribution of OA to OP was assessed. Cox's proportional hazard model showed no significant relationship between the presence of lumbar OA at the baseline and incidence of lumbar and femoral neck OP (lumbar OP, men $P=0.71$, women $P=0.79$; femoral neck OP, women $P=0.52$). Then, the association between lumbar OA and the cumulative incidence of VFx was determined by logistic regression analysis. As reported elsewhere, the cumulative incidence of VFx including subjects with previous VFx in their 40s, 50s, 60s, and 70s was 2.1%, 8.3%, 10.0%, and 12.2% for men and 2.1%, 6.1%, 18.0%, and 22.0% for women, respectively [26]. There was no significant relationship between the presence of lumbar OA at the baseline and incidence of VFx in men and women (men $P=0.21$, women $P=0.64$).

Secondly, the contribution of OP to OA was examined (Table 3). A significant relationship existed between the presence of lumbar OP at the baseline and cumulative incidence of lumbar OA in women ($P<0.05$) but not in men ($P=0.07$). Similarly, there was significant association between lumbar BMD at the baseline and the cumulative incidence of lumbar OA in women (vs. +1 SD, $P<0.05$) but not in men ($P=0.25$). No significant association was identified between femoral neck OP and BMD at the baseline and cumulative incidence of lumbar OA in men and women (OP at femoral neck, women $P=0.32$; BMD at femoral neck, vs. +1 SD, men $P=0.23$, women $P=0.77$). These results indicate that the presence of lumbar OP at the baseline would prevent the occurrence of lumbar OA, and conversely, high lumbar BMD would accelerate the progression of lumbar OA in women.

Finally, the association between the presence of VFx at the baseline and cumulative incidence of lumbar OA was assessed. As shown elsewhere, the prevalence of VFx in the present cohort among men in their 40s, 50s, 60s, and 70s was 4.3%, 14.6%, 22.0%, and 24.5% and that among women was 2.1%, 10.2%, 14.0%, and 44.9%, respectively [27]. Logistic regression analysis showed that there was no significant relationship between the presence of previous VFx and the incidence of lumbar OA in men and women (men $P=0.72$, women $P=0.91$; Table 3).

Discussion

The present study is a 10-year follow-up study of a population-based cohort of Japanese middle-aged people and elderly who were assessed for lumbar OP and OA. We clarified the prevalence of lumbar OP and OA and its trend of changes as well as the incidence of lumbar OP and cumulative incidence of lumbar OA. As for causal relationship, the presence of lumbar OA did not increase the risk of lumbar OP in both genders. However, the presence of lumbar OP significantly reduced the risk of lumbar OA, and high lumbar BMD values would accelerate the occurrence of lumbar OA over 10 years in women, while the presence of OP and BMD at the femoral neck did not influence the occurrence of lumbar OA.

The prevalence of lumbar OP in both 1990 and 2000 was significantly higher in women than in men ($P<0.001$) and gradually increased with age. Regarding the trend of changes in the prevalence of lumbar OP between 1990 and 2000 in same-age groups, no significant difference was shown in both men and women. We previously reported that both men and women in later birth cohorts showed higher BMDs in their middle age in this cohort [25]. However, we failed to clarify any significant decrease in the prevalence of lumbar OP in same-age groups of younger birth cohorts in the present study, although the prevalence

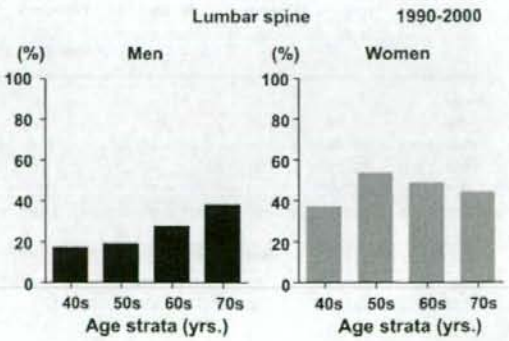

Fig. 3 Cumulative incidence of osteoarthritis at the lumbar spine over 10 years by age group and gender

Table 3 Causal relationship between osteoporosis (OP) and osteoarthritis (OA)

Baseline	Outcome	Reference	Gender	Risk ratio	95% CI	*P* value
Contribution of OA to OP						
OA at lumbar spine	Incidence of OP at lumbar spine	Yes/No	Men	HR 0.76	0.19–3.15	0.71
			Women	HR 0.90	0.40–1.99	0.79
OA at lumbar spine	Incidence of OP at femoral neck	Yes/No	Women	HR 0.74	0.30–1.84	0.52
OA at lumbar spine	Cumulative incidence of VFx	Yes/No	Men	OR 0.41	0.10–1.64	0.21
			Women	OR 1.27	0.46–3.47	0.64
Contribution of OP to OA						
OP at lumbar spine	Cumulative Incidence of OA at lumbar spine	Yes/No	Men	OR 8.68	0.82–92.3	0.07
			Women	OR 0.20	0.05–0.80	0.02
OP at femoral neck	Cumulative Incidence of OA at lumbar spine	Yes/No	Women	OR 0.52	0.14–1.89	0.32
BMD at lumbar spine	Cumulative incidence of OA at lumbar spine	+1 SD	Men	OR 0.80	0.54–1.17	0.25
			Women	OR 1.87	1.16–2.99	0.01
BMD at femoral neck	Cumulative incidence of OA at lumbar spine	+1 SD	Men	OR 0.80	0.56–1.15	0.23
			Women	OR 0.92	0.53–1.60	0.77
VFx	Cumulative incidence of OA at lumbar spine	Yes/No	Men	OR 0.79	0.21–2.95	0.72
			Women	OR 0.91	0.19–4.36	0.91

All analyses were adjusted for age and weight at the baseline
OA at lumbar spine was defined as the KL grade ≥3
BMD bone mineral density, *VFx* vertebral fracture, *SD* standard deviation, *HR* hazard ratio, *OR* odds ratio, *CI* confidence interval

of lumbar OP in 2000 tended to be lower than that in 1990 for all identical age groups in women. This might be explained by the effect of the time gap between the decrease in BMD and occurrence of lumbar OP. Although higher BMD was observed in the middle-aged group, this might not influence epidemiological indices of lumbar OP such as prevalence within only a 10-year span. As participants become old enough to be expected to have lumbar OP, its prevalence is expected to decrease.

Contrary to lumbar OP, the prevalence of lumbar OA was not significantly different between men and women in 1990 and 2000, and age was not associated with the prevalence of lumbar OA except for women in 2000 ($P<0.01$). Regarding the trend of changes in the prevalence of lumbar OA between 1990 and 2000 in same-age groups, the prevalence of lumbar OA in 2000 was higher than that in 1990 in both men and women, with significance in men (men $P<0.01$, women $P=0.08$). Concerning the association between age and lumbar OA, Lawrence found that the radiological prevalence of disc degeneration in the lumbar spine in the age group of 35–45 years increased with age [28]. O'Neill et al. reported that the frequency of vertebral osteophytes increased with age [29]. We previously compared the prevalence of lumbar OA determined by KL grade ≥3 in British and Japanese populations and reported that prevalence was higher in Britain than in Japan [15]. The difference may be partly explained by ethnic variation.

To the best of our knowledge, the present study represents the first report on the incidence of lumbar OP in Japan. If the incidence obtained in this study is generalized to the current Japanese population in the age group of 40–79 years, 970,000 new cases of lumbar OP (160,000 men, 810,000 women) are estimated to occur annually. When classified by age, the incidence of lumbar OP in women was the highest in their 50s, followed by those in their 70s. We previously reported that the rate of change in lumbar spine BMD in women in the present population was the highest in their 50s [12, 25] and is related to the decrease in female hormones [30]. The present finding that the incidence of lumbar OP was the highest among women in their 50s suggests that the incidence of lumbar OP is closely related to the menstrual status, particularly menopause, and rate of change in lumbar spine BMD. Since more than 2.2% of women are estimated to develop lumbar OP annually in their 60s and 70s (ages at which the effects of menopause are thought to be attenuated), measures for preventing lumbar OP among the elderly as well as women during perimenopause are urgently required. The annual incidence of lumbar OP among men in their 60s and 70s was more than 1.0%. Although this incidence is lower than that among women, it is estimated that 160,000 male cases occur annually as previously mentioned, which nevertheless should not be ignored. Predictors for finding early and/or potential lumbar OP in both women and elderly men need to be established immediately.

In addition, we determined the cumulative incidence of lumbar OA with disc space narrowing for the first time in Japan. The 10-year cumulative incidence of lumbar OA with KL grade ≥3 tended to increase with age in men, but not in women, and it was higher in women than in men. Few reports have described the incidence of lumbar OA in

population-based cohorts. Hassett et al. showed that the progression rates for anterior osteophytes and disc space narrowing were 4% and 3% per year, respectively, among female participants in the Chingford study [31], which was approximately similar to the results of the present study. However, since epidemiological indices such as prevalence and incidence are highly dependent on the definition of OA, we cannot compare our results directly with those of other studies. For example, we defined lumbar OA as KL grade ≥3, which shows disc space narrowing with or without osteophytes, while the Chingford study determined lumbar OA based on the grading system of osteophytes and disc space narrowing reported by Lane et al. [32]. Since few reports have investigated the incidence of lumbar OA in the general population, further studies are needed to verify ethnic and geographical differences in the incidence of lumbar OA. When classified by age, the cumulative incidence of lumbar OA and OP was highest in women in their 50s during the early postmenopausal period. Therefore, it might be suggested that endogenous sex steroids play a role in the occurrence or progression of lumbar OA in women.

In some population-based prospective studies, OA of extremities was reported to increase the risk of osteoporotic fractures. In the Rotterdam study, knee OA increased the risk of vertebral and non-vertebral fractures [33]. Arden et al. reported that patients with knee OA and knee pain have an increased risk of hip and other non-vertebral fractures, which was not explained by the increased risk of falls [34]. Intervertebral disc space narrowing was found to increase the risk of VFx in the OFELY study [16, 17]. These findings suggest that OA is involved in the onset of fractures resulting from OP. Conversely, Roux et al. reported that intervertebral disc space narrowing and osteophytes decreased the prevalence of VFx in postmenopausal women with OP [35]. In the present study, there was no significant association between the presence of lumbar OA and future occurrence of lumbar OP and VFx. Lumbar OP is diagnosed by lumbar BMD (the value of which is easily affected by osteophytes and sclerosis of vertebrae and facets and the calcification of abdominal aorta [36]), which can artifactually increase BMD. Therefore, lumbar BMD might not be a good surrogate index of OP. As this is the first report about the causal relationship of lumbar OA and OP in the Japanese population, the difference might be partly due to the ethnic variation between Western and Oriental populations. Further studies are necessary to confirm the causal relationship of OA and OP in Japan and other countries.

Regarding the contribution of OP to OA, we elucidated that OP at the lumbar spine reduced the risk for the progression of lumbar OA in women while high BMD at the lumbar spine accelerated this progression. Zhang et al. found that higher BMD at the hip was associated with prevalent and incident knee OA in older women in the Framingham study [37]. They also found that increased BMD over the follow-up period indicated a high risk of incident knee OA [37]. Hart et al. confirmed that, for women that developed incident knee OA, BMD was higher in the Chingford study [38]. Although these studies reported findings on the BMD and OA at extremities, not the spinal OP and OA, our results were almost similar to those of the above-mentioned cohort studies. Further prospective cohort studies with a larger sample size and longer observational periods are required to conclude the causal relationship of OP and OA.

Contrary to lumbar OP, no causal relationship was observed between OP or BMD at the femoral neck and cumulative incidence of lumbar OA. This might be because OP was diagnosed at different sites, which might have diluted the influence of OA occurrence. This hypothesis will be clarified in a study of the association between OP at the femoral neck and hip OA.

The presence of VFx at baseline showed no association with occurrence of lumbar OA. The prevalence of VFx includes various causes, and not all VFx were caused by OP. The geographic area in which the present cohort was established is mountainous, and a significant number of male subjects worked in the forestry industry and had experienced falls from trees or down slopes accidentally. In addition, most participants with previous VFx at the baseline were old and did not complete the 10-year follow-up. This survival bias might have influenced the evaluation of the influences of VFx on occurrence of OA.

The inverse causal relationship between lumbar OP and OA was only observed in women, not in men. These gender differences might be explained partly by differences in the incidence of lumbar OP. The incidence in men in the present study might be insufficient to detect the causal relationship. Alternatively, differences in gender-dependent factors such as endogenous sex steroids could influence the association of OP and OA.

There are several limitations in this study. The primary limitation is that the cohort comprised a relatively small number of participants. We were able to follow male and female residents with confirmed regional representativeness for 10 years with a high participation rate of 74.8%. However, 101 participants were lost in the follow-up study during the 10 years. The main reason for them dropping out of the study was death. The mean age of women completers of the age group 70-79 was significantly younger than that of drop-outs. Therefore, the prevalence of lumbar OP and cumulative incidence of lumbar OA in this age group might be underestimated due to the effects of survival bias. A secondary limitation is related to the definition of lumbar OA. Cumulative incidence as used in the present study was

detected by dividing the number of individuals who developed new lumbar OA by the number of participants in the follow-up study. Individuals with previous lumbar OA were excluded from both the numerators and denominators. In this formula, we excluded 69 male and 70 female participants with lumbar OA at the baseline to obtain the incidence of the first lumbar OA, which might reduce the total number of population at risk and cause a decrease in statistical power. Our result regarding lumbar OA incidence in the present study might need to be confirmed in larger population-based cohorts.

With the goal of elucidating the environmental and genetic background of bone and joint diseases represented by OA and OP, we established larger scale cohorts based on the present cohort, called Research on Osteoarthritis/Osteoporosis Against Disability (ROAD), and have already started the follow-up study [39]. This enlarged population-based cohort study may confirm the consistency of epidemiological trends for OP and OA and clarify the causal relationship between these two major bone and joint diseases.

Conclusion

Based on observations from a population-based cohort over a 10-year period, the estimated incidence of OP at the L2–4 level of the lumbar spine per 10,000 person-years for men in their 40s, 50s, 60s, and 70s was 0, 0, 109.5, and 151.1 and that for women was 124.2, 384.0, 227.3, and 239.5, respectively. The cumulative incidence of lumbar OA over 10 years for men in their 40s, 50s, 60s, and 70s was 18.5%, 20.0%, 27.6%, and 37.9% for men and 37.1%, 53.6%, 48.4%, and 43.8% for women, respectively. Cox's proportional hazards model showed no significant relationship between the presence of lumbar OA at the baseline and future incidence of lumbar and femoral neck OP. A significant relationship existed between the presence of lumbar OP at the baseline and future incidence of lumbar OA in women (odds ratio 0.20, 95% confidence interval 0.05–0.80, $P<0.05$). It may be suggested that the presence of OA does not increase the risk of incident OP in both genders and that the presence of OP reduces the risk of incident OA at the spine in women.

Acknowledgments This study was supported by Grants-in-Aid for Scientific Research B20390182 (Noriko Yoshimura), C20591737 (Toru Akune), C20591774 (Shigeyuki Muraki), Young Scientists A18689031 (Hiroyuki Oka), and Collaborating Research with NSF 08033011-00262 (Noriko Yoshimura) from the Ministry of Education, Culture, Sports, Science and Technology, H17-Men-eki-009 (Director, Kozo Nakamura), H18-Choujyu-037 (Director, Toshitaka Nakamura), and H20-Choujyu-009 (Director, Noriko Yoshimura) from the Ministry of Health, Labour and Welfare in Japan. This study was also supported by grants from the Japan Osteoporosis Society, Japan Health Foundation, Nakatomi Foundation (Noriko Yoshimura), and research aid from the Japanese Orthopaedic Association (Director, Hiroshi Kawaguchi). The authors wish to thank Mrs. Tomoko Takijiri, Mrs. Kumiko Shinou, Mr. Kenji Kubo, and other members in the public office in Miyama village for their assistance and scheduling participants for examinations.

Conflicts of interest None.

References

1. Yamamoto I (1999) Estimation for the number of patients of osteoporosis in Japan. Osteoporosis Jpn 7:10–11 (in Japanese)
2. Ministry of Health, Labour and Welfare. Outline of the results of National Livelihood Survey 2004. http://www.mhlw.go.jp/toukei/saikin/hw/k-tyosa/k-tyosa04/4-2.html
3. Muraki S, Yamamoto S, Ishibashi H, Nakamura K (2006) Factors associated with mortality following hip fracture in Japan. J Bone Miner Metab 24:100–104
4. Jornell O, Kanis JA, Oden A, Sembo I, Redlund-Johnell I, Petterson C, De Laet C, Jonsson B (2004) Mortality after osteoporotic fractures. Osteoporosis Int 15:38–42
5. Sambrook P, Naganathan V (1997) What is the relationship between osteoarthritis and osteoporosis? Baillieres Clin Rheumatol 11:695–710
6. Dequecker J, Boonen S, Aerssens J, Westhovens R (1996) Inverse relationship osteoarthritis–osteoporosis: what is the evidence? What are the consequences? Br J Rheumatol 35:813–818
7. Dequecker J, Aerssens J, Luyten FP (2003) Osteoarthritis and osteoporosis: clinical and research evidence of inverse relationship. Aging Clin Exp Res 15:426–439
8. Jones G, Nguyen T, Sambrook PN, Lord SR, Kelly PJ, Eisman JA (1995) A longitudinal study of the effect of spinal degenerative disease on bone density in the elderly. J Rheumatol 22:932–936
9. Liu G, Peacock M, Eilam O, Dorulla G, Braunstein E, Johnston CC (1997) Effect of osteoarthritis in the lumbar spine and hip bone mineral density and diagnosis of osteoporosis in elderly men and women. Osteoporos Int 7:564–569
10. Hart DJ, Mootoosamy I, Doyle DV, Spector TD (1994) The relationship between osteoarthritis and osteoporosis in the general population: the Chingford study. Ann Rheum Dis 53:158–162
11. Belmonte-Serrano MA, Bloch DA, Lane NE, Michel BE, Fries JF (1993) The relationship between spinal and peripheral osteoarthritis and bone density measurements. J Rheum 20:1005–1013
12. Yoshimura N, Hashimoto T, Morioka S, Sakata K, Kasamatsu T, Cooper C (1998) Determinants of bone loss in a rural Japanese community. The Taiji study. Osteoporos Int 8:604–610
13. De Laet C, Kanis JA, Oden A, Johanson H, Johnell O, Delmas P, Eisman JA, Kroger H, Fujiwara S, Garnero P, McCloskey EV, Mellstrom D, Melton LJ 3rd, Meunier PJ, Pols HA, Reeve J, Silman A, Tenenhouse A (2005) Body mass index as a predictor of fracture risk: a meta-analysis. Osteoporos Int 16:1330–1338
14. Hartz AJ, Fischer ME, Bril G, Kelber S, Rupley D Jr, Oken B, Rimm AA (1986) The association of obesity with joint pain and osteoarthritis in the HANES data. J Chronic Dis 39:311–319
15. Yoshimura N, Dennison E, Wilman C, Hashimoto T, Cooper C (2000) Epidemiology of chronic disc degeneration and osteoarthritis of the lumbar spine in Britain and Japan: a comparative study. J Rheumatol 27:429–433
16. Sornay-Rendu E, Munoz F, Duboeuf F, Delmas PD (2004) Disc space narrowing is associated with an increased vertebral fracture

risk in postmenopausal women: the OFELY Study. J Bone Miner Res 19:1994–1999
17. Sornay-Rendu E, Allard C, Munoz F, Duboeuf F, Delmas PD (2006) Disc space narrowing as a new risk factor for vertebral fracture: the OFELY study. Arthritis Rheum 54:1262–1269
18. Kasamatsu T, Morioka S, Hashimoto T, Kinoshita H, Yamada H, Tamaki T (1991) Epidemiological study on bone mineral density of inhabitants in Miyama Village, Wakayama Prefecture (Part 1). Background of study population and sampling method. J Bone Miner Metab 9(suppl):50–55
19. Kinoshita H, Danjoh S, Yamada H, Tamaki T, Kasamatsu T, Ueda A, Hashimoto T (1991) Epidemiological study on the bone mineral density of inhabitants in Miyama Village, Wakayama Prefecture (part II). Bone mineral density of the spine and proximal femur. J Bone Miner Metab 9(suppl):56–60
20. Yoshimura N, Kakimoto T, Nishioka M, Kishi T, Iwasaki H, Niwa T, Morioka S, Sakata T, Hashimoto T (1997) Evaluation of reproducibility of bone mineral density measured by dual energy X-ray absorptiometry (Lunar DPX-L). J Wakayama Medical Society 48:461–466
21. World Health Organization (1994) Assessment of fracture risk and its application to screening for postmenopausal osteoporosis. WHO technical report series 843. WHO, Geneva
22. Orimo H, Hayashi Y, Fukunaga M, Sone T, Fujiwara S, Shiraki M, Kushida K, Miyamoto S, Soen S, Nishimura J, Oh-Hashi Y, Hosoi T, Gorai I, Tanaka H, Igai T, Kishimoto H (2001) Osteoporosis Diagnostic Criteria Review Committee: Japanese society for bone and mineral research. Diagnostic criteria for primary osteoporosis: year 2000 revision. J Bone Miner Metab 19:331–337
23. Kellgren JH, Lawrence LS (1957) Radiological assessment of osteo-arthrosis. Ann Rheum Dis 16:494–502
24. Inoue T (1990) Clinical features and findings, osteoporosis (in Japanese). Bone 4:39–47
25. Yoshimura N, Kinoshita H, Danjoh S, Takijiri T, Morioka S, Kasamatsu T, Sakata K, Hashimoto T (2002) Bone loss at the lumbar spine and the proximal femur in a rural Japanese community, 1990–2000: the Miyama study. Osteoporos Int 13:803–808
26. Yoshimura N, Kinoshita H, Oka H, Muraki S, Mabuchi A, Kawaguchi H, Nakamura K (2006) Cumulative incidence and changes in prevalence of vertebral fractures in a rural Japanese community: a 10-year follow-up of the Miyama cohort. Arch Osteoporos 1:43–49 doi:10.1007/s11657-006-0007-0
27. Yoshimura N, Kinoshita H, Danjoh S, Yamada H, Tamaki T, Morioka S, Kasamatsu T, Hashimoto T, Inoue T (1995) Prevalence of vertebral fractures in a rural Japanese population. J Epidemiol 5:171–175
28. Lawrence JS (1969) Disc degeneration. Its frequency and relationship to symptoms. Ann Rheum Dis 28:121–138
29. O' Neill TW, McCloskey EV, Kanis JA, Bhalla AK, Reeve J, Reid DM, Todd C, Woolf AD, Silman AJ (1999) The distribution, determinants, and clinical correlates of vertebral osteophytosis: a population based survey. J Rheumatol 26:842–848
30. Yoshimura N, Kasamatsu T, Sakata K, Hashimoto T, Cooper C (2002) The relationship between endogenous estrogen, sex hormone binding globulin and bone loss in female residents of a rural Japanese community: the Taiji study. J Bone Miner Metab 20:303–310
31. Hassett G, Hart DJ, Manek NJ, Doyle DV, Spector TD (2003) Risk factors for progression of lumbar spine disc degeneration, the Chingford study. Arthritis Rheum 48:3112–3117
32. Lane N, Nevitt MC, Genant HK, Hochberg MC (1993) Reliability of new indices of radiographic osteoarthritis of the hand and hip and lumbar disc degeneration. J Rheumatol 20:1911–1918
33. Bergink AP, van der Klift M, Hofman A, Verhaar JA, van Leeuwen JP, Uitterlinden AG, Pols HA (2003) Osteoarthritis of the knee is associated with vertebral and nonvertebral fractures in the elderly: the Rotterdam study. Arthritis Rheum 49:648–657
34. Arden NK, Croziew S, Smith H, Anderson F, Edwards C, Raphael H, Cooper C (2006) Knee pain, knee osteoarthritis, and the risk of fracture. Arthritis Rheum 55:610–615
35. Roux C, Fechtenbaum J, Briot K, Cropet C, Liu-Lèage S, Marcelli C (2008) Inverse relationship between vertebral fractures and spine osteoarthritis in postmenopausal women with osteoporosis. Ann Rheum Dis 67:224–228
36. Kinoshita H, Tamaki T, Hashimoto T, Kasagi F (1998) Factors influencing lumbar spine bone mineral density assessment by dual energy X-ray absorptiometry: comparison with lumbar spinal radiogram. J Orthop Sci 3:3–9
37. Zhang Y, Hannan MT, Chaisson CE, McAlindon TE, Evans SR, Aliabadi P, Levy D, Felson DT (2000) Bone mineral density and risk of incident and progressive radiographic knee osteoarthritis in women: the Framingham study. J Rheumatol 27:1032–1037
38. Hart DJ, Cronin C, Daniels M, Worthy T, Doyle DV, Spector TD (2002) The relationship of bone density and fracture to incident and progressive radiographic osteoarthritis of the knee: the Chingford Study. Arthritis Rheum 46:92–99
39. Muraki S, Oka H, Mabuchi A, Akune T, En-yo Y, Yoshida M, Saika A, Suzuki T, Yoshida H, Ishibashi H, Yamamoto S, Nakamura K, Kawaguchi H, Yoshimura N (2008) Prevalence of radiographic lumbar spondylosis and its association with low back pain in the elderly of population-based cohorts: the ROAD study. Ann Rheum Dis (in press)

Ultrasound in Med. & Biol., Vol. 34, No. 5, pp. 775–783, 2008

0301-5629/08/$–see front matter

ELSEVIER

doi:10.1016/j.ultrasmedbio.2007.11.005

● *Original Contribution*

A NEW METHOD FOR EVALUATION OF FRACTURE HEALING BY ECHO TRACKING

JUNTARO MATSUYAMA,* ISAO OHNISHI,* RYOICHI SAKAI,† MASAHIKO BESSHO,* TAKUYA MATSUMOTO,* KOICHI MIYASAKA,† AKIMITSU HARADA,† SATORU OHASHI,* AND KOZO NAKAMURA*

*Department of Orthopaedic Surgery, University of Tokyo and †Research Laboratory, Aloka Co. Ltd., Tokyo, Japan

Abstract—Assessment of bone healing on radiographs depends on the volume and radio-opacity of callus at the healing site, but is not necessarily objective, and there are differences of judgment among observers. To overcome this disadvantage, a clinical system was developed to quantify the stiffness of healing fractures of the tibia in patients by the echo tracking (ET) method in a manner similar to a three-point bending test. The purpose of this study was to ensure that the ET system could clinically assess the progress, delay or arrest of healing. The fibular head and the lateral malleolus were supported. A 7.5-MHz ultrasound probe was placed on the proximal and distal fragments and a load of 25 N was applied. Five tracking points were set along the long axis of the ultrasound probe at intervals of 10 mm. With a multiple ET system, two probes measured the displacement of five tracking points on each of the proximal and distal fragments of the tibia, thereby detecting the bending of the two fragments generated by the load. ET angle was defined as the sum of the inclinations of the proximal and distal fragments. Eight tibial fractures in seven patients treated by a cast or internal fixation were measured over time. In patients with radiographically normal healing, the bending angle decreased exponentially over time. However, in patients with nonunion, the angle remained the same over time. It was demonstrated that the ET method could be clinically applicable to evaluate fracture healing as a versatile, quantitative and noninvasive technique. (E-mail: ohnishii-dis@h.u-tokyo.ac.jp) © **2008 World Federation for Ultrasound in Medicine & Biology.**

Key Words: **Ultrasound, Echo tracking, Fracture site stiffness, Fracture healing.**

INTRODUCTION

The most important issue in assessment of fracture healing is to obtain information about restoration of the mechanical integrity of the bone. In clinical practice, fracture healing is usually judged from serial radiographs. Assessment of bone healing on radiographs depends on the volume and radio-opacity of callus at the healing site, but is not necessarily objective, and there are differences of judgment among observers. In addition, radiographs cannot evaluate fracture site strength. In these respects, assessment of fracture healing by using radiographs is far from ideal.

The stated disadvantages of radiography for assessment of fracture healing have been pointed out in recent years, and various other methods of assessment have been developed. Jernberger (1970) devised an invasive method for measuring the bending stiffness of healing fractures of the tibia. With his method, the proximal and distal bone fragments were fixed by screws that were connected to a specially designed beam, and a load was applied through a screw at the center of the fixing screws. The method was based on the principle governing the bending of two beams connected at the ends and subjected to a bending force applied at the midpoint. Burny et al. (1984) developed a method that used a strain gauge attached to a fixator shaft. With their method, the strain gauge readings were monitored over time during weight bearing, and the pattern of fracture healing was classified into seven categories (such as normal, delayed, arrested, *etc.*). Assessment using acoustic emission (AE) was developed by Nicholls and Berg (1981), who detected acoustic pulses generated by microscopic failure of the bone under loading. The investigation by Watanabe et al. (2001) revealed that AE signals occurred with the yielding of callus. However, the strain gauge method and the AE method have the disadvantage that both are limited to patients with external fixation, and both require the in-

Address correspondence to: Isao Ohnishi, M.D., Ph.D., Department of Orthopaedic Surgery, University of Tokyo, 7–3–1 Hongo, Bunkyo-ku Tokyo, 113–0033, Tokyo, Japan.
E-mail: ohnishii-dis@h.u-tokyo.ac.jp

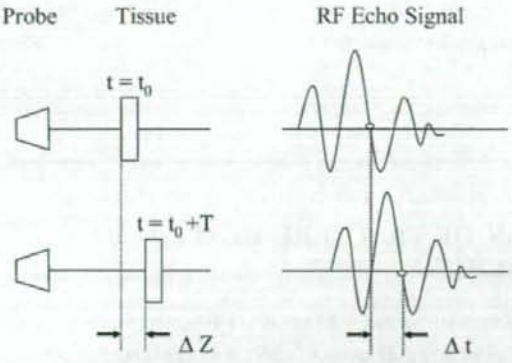

Fig. 1. The target tissue may move closer to or away from an ultrasonic probe over the distance ΔZ during a pulse repetition time of ultrasonic waves (T), causing phase delay of the RF echo signal (Δt). The ET method measures the extent of this displacement by tracking the initialized phase pattern of the echo signal.

sertion of screw pins or wires. For these reasons, such methods have not been widely used and a new method is needed that is both noninvasive and widely applicable.

To overcome such limitations, we developed a new method for the noninvasive and quantitative assessment of fracture healing. Bone always undergoes deformation in response to an applied load. By quantitatively measuring this deformation, it is possible to assess the mechanical properties of bone and thereby estimate the strength of a fracture site. In this study, we attempted to noninvasively assess the bending stiffness of the healing fracture sites after applying a load. To measure bending stiffness, we focused on ultrasound because it is noninvasive. Precise measurement of the displacement of a specific point can be done by the echo tracking (ET) method. This method is a technique for measuring minute displacement of a certain point on a tissue by detecting a wave pattern in the radiofrequency (RF) echo signal reflected from the target tissue (Fig. 1) (Hokanson et al. 1972). To apply this technique for detection of bone deformation, we improved it so that displacement could be measured with an accuracy of 2.6 μm (Matsuyama et al. 2006). We also developed a multi-ET system that was able to simultaneously track dynamic movement at multiple points on the bone surface. In our previous study of the three-point bending test using a porcine tibia, the strain gauge readings and the data from the multi-ET system showed an almost perfect linear correlation with the load ($r = 0.998$). These results indicated the possibility of using the echo tracking method to detect bone surface deformation.

The purpose of this study was to determine whether our newly developed ET system could clinically assess the progress, delay or arrest of healing by detecting the bending stiffness at the fracture healing site. Fracture healing was evaluated in patients with tibia fracture treated by a cast or internal fixation.

METHODS

A clinical system was developed to quantify the stiffness of healing fractures of the tibia in patients by the ET method in a similar manner to a three-point bending test. Five tracking points were set along the long axis of the ultrasound probe at intervals of 10 mm. With a multiple ET system, two probes measured the displacement of five tracking points on each of the proximal and distal fragments of the tibia, thereby detecting the bending of the two fragments generated by the load. ET angle was defined as the sum of the inclinations of the proximal and distal fragments (Fig. 2). When callus was weak in the initial stage of healing, the tracked points were almost in a straight line and the inclination of the two fragments was calculated directly. However, when the callus was more rigid in the late stage of healing, the line connecting the points was curved and the inclination was obtained from the slope of the linear regression equation for the displacement of the points.

Before clinical application of this method, its accuracy was evaluated by measuring the inclination of the metal flat panel.

Measurement of the accuracy of ET angle using an inclined flat metal panel

A flat stainless steel (SUS 420J) panel (length 270 mm, width 60 mm, thickness 5 mm) was used, which had a parallel accuracy and flatness variation of <2 μm. One end of the panel was attached to a magnet stand (DG, Noga Japan Ltd, Saitama, Japan), and the other side was attached to a goniometer (X13–001, Tsukumo Co. Ltd, Saitama, Japan) fixed to another magnet stand. Then, the

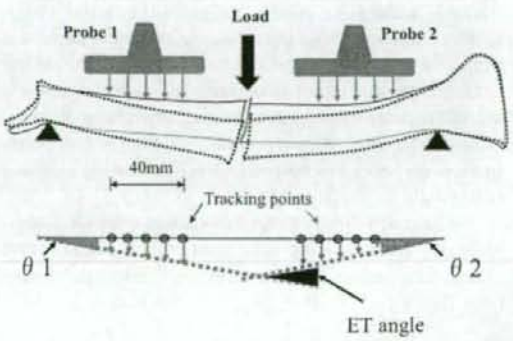

Fig. 2. Probes are set on each of the proximal and distal fragments of the tibia to detect the bending of the two fragments generated by a load. The ET angle is defined as the sum of the inclination of both fragments.

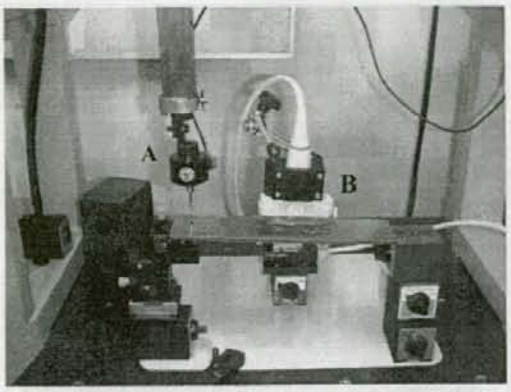

Fig. 3. The accuracy of the ET measurement was evaluated by measuring the inclination of the flat metal panel simultaneously using a 3-D measuring device. (A) 3-D measuring device; (B) 7.5-M Hz linear ultrasound probe.

metal panel was inclined by increasing the height of the goniometer stand. A 7.5-M Hz linear ultrasound probe (UST-5710-7.5, Aloka Co. Ltd., Tokyo) was set at a distance of 20 mm from the panel to measure the changes of displacement of each of five points on the panel (Fig. 3). Using these data, the ET angle of the panel was calculated. At the same time, the inclination of the panel was accurately measured using a 3-D measuring device (AE112, Mitsutoyo, Kanagawa, Japan) with an accuracy of 1 μm. The panel was inclined by elevating the sliding mechanism of the stand by 0.4 mm and the inclination of the panel was measured 5 times, after which the mean and standard deviation were calculated. Accuracy was evaluated by calculating the standard deviation of the difference between the ET angle and the inclination measured by the 3-D measuring device in each of the measurement trials.

Clinical measurement of fracture site bending stiffness

Eight tibial fractures in seven patients with an average age of 37 y (range 24–69 y) were measured (Table 1). Two fractures of two patients were treated conservatively with a cast, and six fractures of five patients were treated by internal fixation (locked intramedullary nailing in 4, plating in 1 and screws in 1). The average measurement period was 40.8 wk (21–60 wk), and the average number of measurements was 7.5 (5–11).

Patients assumed the supine position with both knees extended, and the affected leg was held horizontal with the antero-medial aspect of the tibia upwards. The fibular head and the lateral malleolus were supported and held tight by a Vacufix (Muranaka Medical Instrument Co., Ltd., Osaka, Japan) to avoid rotation of the leg during loading trials. Before measurement, B-mode images of the short axis of the proximal and distal fragments of the tibia were obtained to identify the center in both directions. By connecting both of the centers, the anatomical axis of the tibia was identified. A 7.5-MHz ultrasound probe was placed on the antero-medial aspect of each of the proximal and distal fragments in the long axis. Each probe was equipped with a multi-ET system with five tracking points at 10-mm intervals. The probes were set vertically on the skin of the leg and held tight with an articulated holder (DG61003, Noga Japan Ltd., Saitama, Japan). A load of 25 N was applied at a rate of 5 N/s and then reduced to 0 N at the same rate using a force gauge (DNP, Imada, Osaka, Japan) parallel to the direction of the probe at the most distal part of the proximal fragment adjacent to the fracture site (Fig. 4). For the initial measurement obtained in each patient, the loading point was set right on the long axis near the fracture site using a B-mode image as a guide. With this setup, the tibia was bent in the same way as for a three-point bending test in the direction of the ultrasound beam. In patients with oblique or spiral fractures, the loading point and the tracking points were set so that they did not cover the fracture site. In patients with a bone graft at the fracture site, the loading point was set on the graft, but the probes were placed so as not to cover it. In the patient with a plate, both the proximal and distal probes were set on the plate surface to measure bending of the plate. Using the multi-ET system, the probes

Table 1. Clinical cases of the tibial fracture

Case	Gender	Age	Limb	Treatment fracture healing	Measurement period (Initial-final)	Radiographic finding
1	F	24	L	Casting	4–47 wk	Normal
2	M	29	R	Casting	7–28 wk	Normal
3	M	23	R	Bone grafting	8–27 mo	Normal
4	M	31	R	Nailing	4–39 wk	Normal
5	F	57	R	Nailing	5–10 mo	Normal
6	F	57	L	Nailing	6–10 mo	Normal
7	F	26	R	Nailing	5 y 2 mo–5 y 7 mo	Nonunion
8	M	69	R	Plating	9–45 wk	Delayed

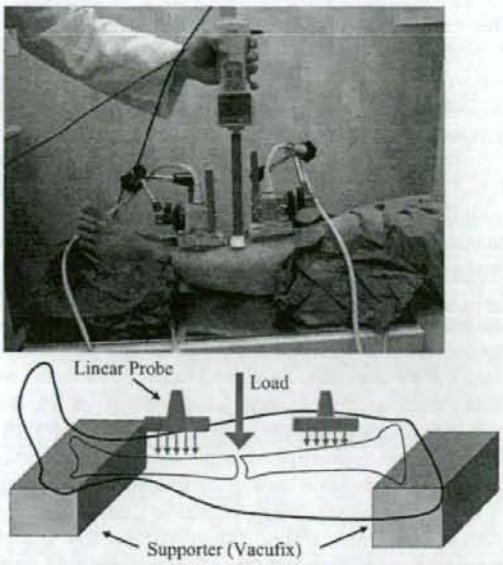

Fig. 4. The affected leg of a patient was held horizontal with the antero-medial aspect of the tibia upwards. The fibular head and the lateral malleolus were supported and held tight by a Vacufix. The probes were set vertically on the skin of the leg and held tight with an articulated arm. A load was applied using a force gauge parallel to the direction of the probe.

detected the angle between the proximal and distal fragments generated by the load. Measurement was repeated five times, and the mean and the standard deviation of the ET angle were calculated.

Fracture healing was assessed at intervals of two or three weeks until radiographic union or arrest of healing occurred. In each patient, the decrease of the ET angle was statistically examined to determine whether it decreased exponentially and whether the decrease was significant. To evaluate the changes of the ET angle over time, exponential regression analysis was performed, and the curve of the ET angle *vs.* time relation was drawn. Differences were considered significant when the p value was less than 0.05.

To investigate the influence of the position of the probes and the patient on the results, the precision of the method was evaluated by repeated measurement of the ET angle in a patient with a diaphyseal fracture of the tibia treated by a cast (case 2). In addition, the linearity of the relation between the load and the ET angle was assessed by incrementally increasing the load from 10 to 30 N. The ultrasound device (SSD 1000, Aloka Co. Ltd.) used in this investigation is used clinically and its safety has been established. The protocol of this investigation was approved by the ethics committee of The University of Tokyo Hospital, and the patients were enrolled after informed consent was obtained.

RESULTS

Accuracy of ET angle measurement for a flat metal panel

Measurement of the inclination of the flat metal panel showed that the average inclination was 0.117° and the standard deviation was 0.002°. The average inclination obtained with the 3-D measuring device was 0.116°, with a standard deviation of 0.003°. The standard deviation of the differences between the data obtained by the ET method and by the 3-D measuring device was 0.002°.

Clinical measurement of fracture site bending stiffness

The average time required for measurement was 17 min (range 15–20 min). At each loading trial, none of the patients complained of pain and there were no complications related to measurement.

The precision of this method was evaluated by repeating measurement of case 2 (treated with a cast), with repositioning of the leg and the ultrasound probes. The mean and standard deviation of the ET angle were 0.316 ± 0.015, and the coefficient of variation was calculated to be 4.6%. The linearity of the relation between the load and the bending angle was very high, with a correlation coefficient of 0.997.

Cases presentation

Case 1: A 24-year-old-woman treated with a cast. The patient sustained a spiral fracture of the proximal diaphysis of the tibia in a traffic accident, and a patella tendon bearing brace cast was applied. Healing was assessed by the ET method, as well as radiographs a total of 11 times from 4 weeks to 47 weeks after fracture. The fracture line became opaque and the callus volume increased from 4 weeks to 19 weeks, but after 26 weeks there was almost no change of the thickness of the callus. On the other hand, measurement showed that the ET angle was about 1° at 4 weeks, and that it decreased exponentially ($y = 1.40e^{-0.105x}$, $r = -0.975$, $p < 0.0001$). The ET angles of both cases 1 and 2 treated with a cast decreased exponentially over time and they reached the level of the intact side by 22 weeks (Fig. 5a, b).

Case 7: A 26-year-old-woman with a fracture of the diaphysis of the tibia treated by a locked intramedullary nailing. ET measurement was performed five times from 5 y 2 mo to 6 y 7 mo after fracture. Her X-ray films showed hypertrophic nonunion, but judgment whether healing was proceeding was extremely difficult. ET measurement showed that there was no significant decrease of the angle over a period of 1 y and 5 mo ($y = 0.264e^{0.002x}$, $r = 0.238$, $p = 0.700$) (Fig. 6a, b).

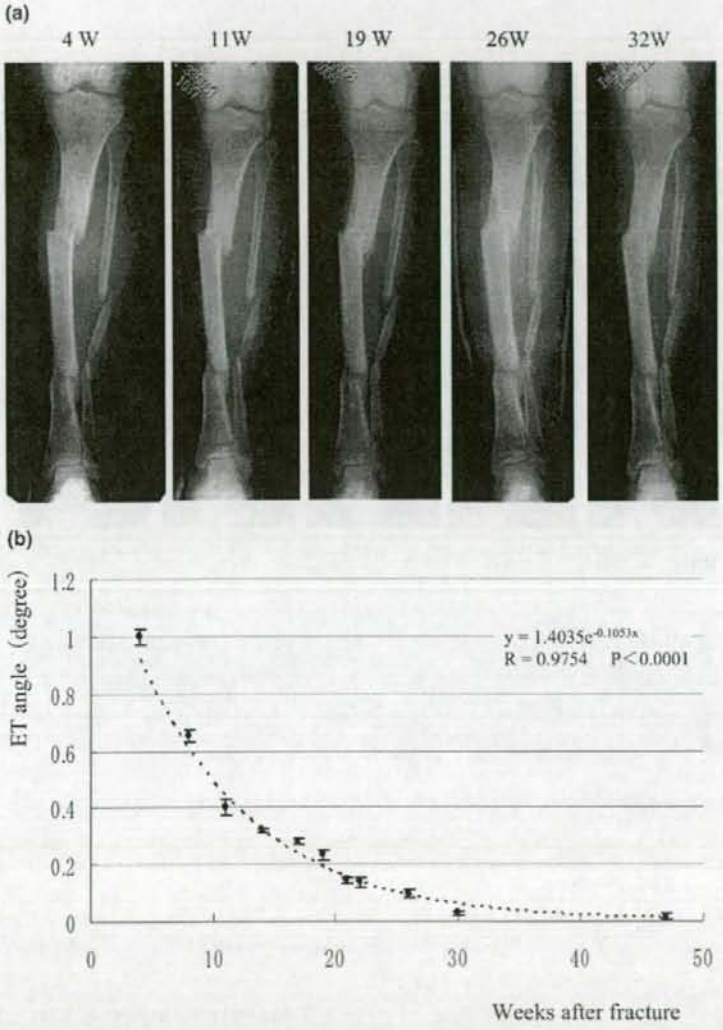

Fig. 5. (a) Time sequential change of the fracture site X-ray from 4 weeks to 32 weeks after fracture in case 1 treated with casting. The fracture site healed normally. (b) In the same patient, the ET angle was plotted. The ET angles decreased exponentially over time.

Case 8: A 69-year-old-man with a long oblique fracture treated with a plate. His X-ray films showed a long oblique fracture line extending for almost 80 mm. Measurement was performed 10 times from 9 weeks to 45 weeks after fracture, during which period almost no change of the fracture site or callus was recognized on X-ray films. The ET method measured the bending angle of the plate. The change was very slow, but the angle decreased significantly from 0.28 to 0.2 degrees, and then finally declined to 0.1 degree. The overall change showed an exponential curve ($y = 0.40e^{-0.030x}$, $r = -0.895$, $p = 0.0005$) (Fig. 7a, b). In patients with radiographically normal healing, the bending angle decreased exponentially over time (Fig. 8). However, in patients with nonunion, the angle remained the same over time.

DISCUSSION

Our method allows noninvasive assessment of bending stiffness at the healing site, so it can be appli-

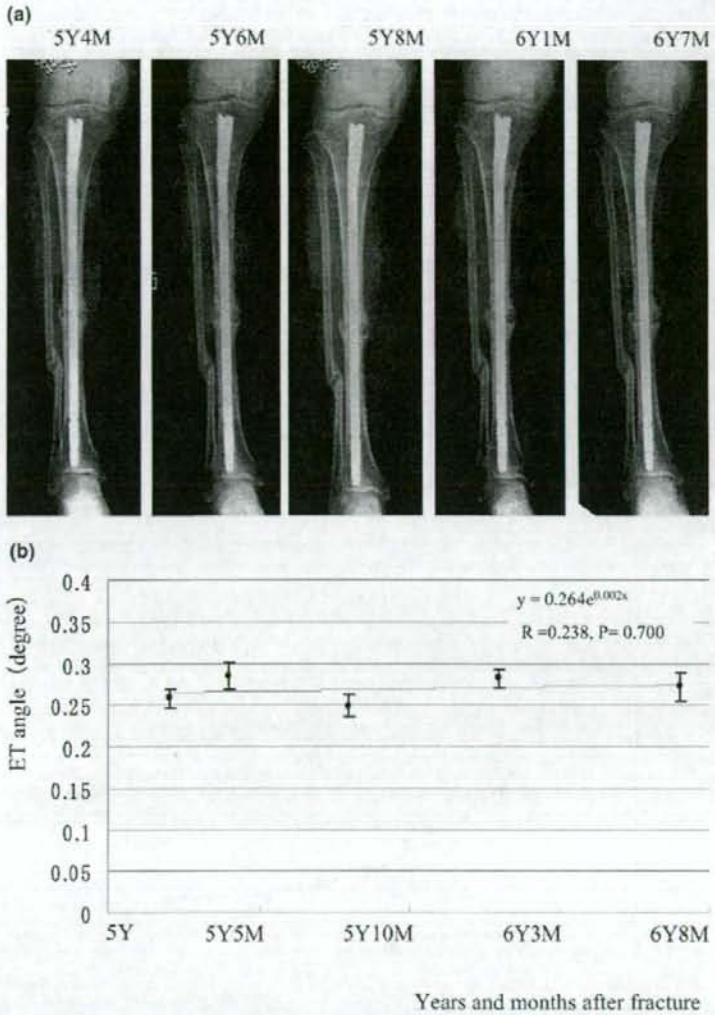

Fig. 6. (a) Time sequential change of the fracture site X-ray from 5 y 4 mo to 6 y 7 mo after fracture in case 7, treated with intramedullary nailing. The X-ray films showed hypertrophic nonunion, but judgment of whether healing was proceeding was extremely difficult. (b) In case 7, the ET angle showed no change over time and the regression lines showed no significant decrease.

cable to patients treated conservatively as well as those managed by surgical intervention with plating or intramedullary nailing.

In this study, the precision and reproducibility of the method were evaluated. The precision of measuring displacement by using the echo tracking system specially designed for bone surface measurement has already been assessed, and a precision of 2.6 μ was demonstrated in our previous study. However, the precision of measuring the bending angle has not been investigated before. We obtained a precision of 0.002°, which was thought to be adequate based on the results of the study by Moorcroft et al. (2001) that evaluated fracture healing. They used the three-point bending test to generate angles of 0.4 to 1.0° in an *in-vivo* measurement trial and connected a goniometer to the bone fragment *via* screw pins fixed to a side bar of the external fixator to detect bending at the fracture site.

When estimation of the linearity of measurement was done in relation to the load, there was excellent

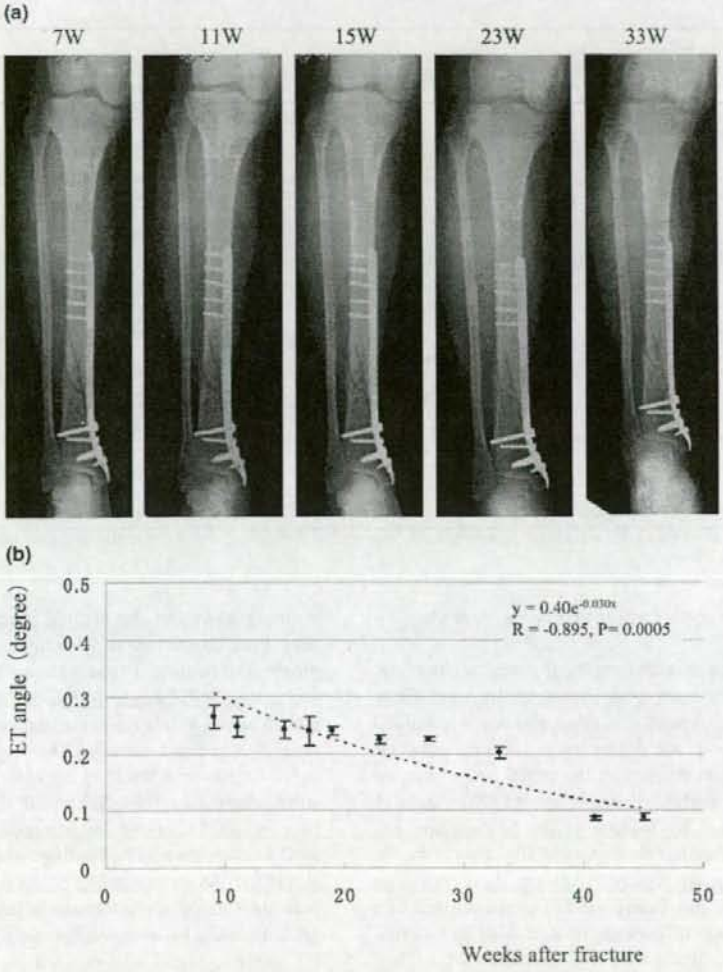

Fig. 7. (a) The X-ray films of case 8, treated with plating. No change of the fracture site or callus was recognized on X-ray films. (b) The ET method measured the bending angle of the plate. The change was very slow, but the angle decreased significantly from 0.28 to 0.2°, and then finally declined to 0.1°.

linearity between magnitude of the load and the ET angle ($r = 0.997$), indicating that elastic deformation of the fracture site had occurred under a load range of 10 to 30 N. Therefore, measurement was shown to be noninvasive as well as safe, without causing any residual deformity.

Reproducibility of the measurement method was estimated to be 0.015°, which was adequate to evaluate fracture healing quantitatively, because the angle ranged from around 1° in the initial stage to about 0.1° in the final stage when it was almost equivalent to that of the intact tibia. However, we have to improve the reproducibility of measurement *in vivo*. The factors affecting reproducibility *in vivo* include the position of the leg, loading direction and positions of the probes. Among these, the positioning or fixation of the leg seems to have the most influence on the reproducibility of measurement.

For clinical evaluation of fracture healing, data obtained by the ET method were compared with X-ray findings over time. In patients with delayed healing or nonunion, judgment of the healing process using X-ray films was difficult because the direction and conditions of obtaining images were not exactly the same every time, so the findings were not reproducible. In contrast, the echo tracking method evaluated fracture stiffness

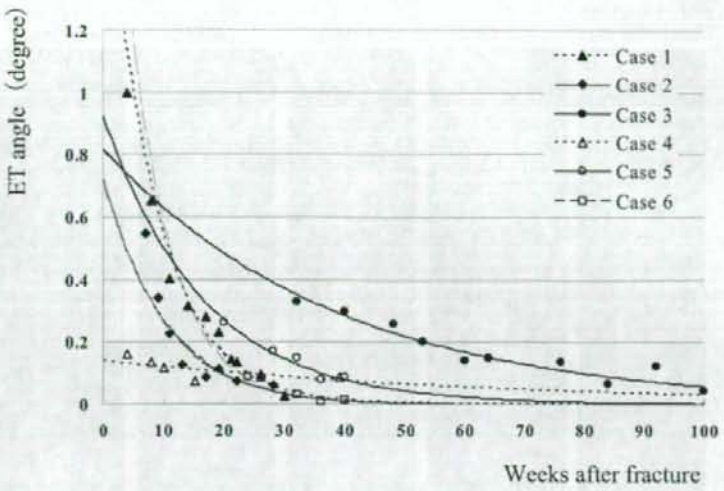

Fig. 8. In cases 1 through 6, the changes of the ET angle showed an exponential pattern. The correlation coefficients obtained by the regression equation for the ET angle and time were very high in these cases.

with considerable accuracy, sensitivity and reproducibility.

In patients with radiographically normal healing, the bending angle decreased exponentially over time. However, in patients with nonunion, the angle remained the same over time. According to the results obtained with previous methods such as the strain gauge method and the invasive method of Jernberger (1970), strain or deformation caused by loading at the healing site has been reported to diminish exponentially over time in patients with normal healing. Among these previous studies, Bourgois and Burny (1972) evaluated fracture healing in hundreds of patients treated with an external fixator that was instrumented with a strain gauge. They not only accumulated considerable clinical data on the strain readings over time, but also theoretically proved by mathematical simulation that the change of the strain over time during normal healing could be expressed as a typical hyperbolic curve. In addition to this, they proved that the time course of the change in strain could also be a hyperbolic curve by developing fracture simulation models with stabilization by intramedullary nailing, plating and external fixation. As a result, their clinical data were compatible with those for the theoretical model of external fixation. They classified the pattern of fracture healing into seven categories depending on the difference in the healing process. Among them, normal healing was defined as healing in which the strain reading *vs.* time curve reaches a plateau at 60 to 90 days after fracture. Slow healing was defined as healing in which the decline of strain was very slow compared with the normal pattern but the healing process was progressive over time. Nonunion was defined as cessation of the progress of healing. In two patients treated with a cast in our study, the ET angle decreased rapidly until 10 weeks after fracture to a level twice that on the intact side, and then it decreased slowly. The exponential regression curve for the echo tracking angle *vs.* time showed a very strong correlation (case 1, $r = -0.975$). Therefore, it can be concluded that the echo tracking method could be used to evaluate normal healing as proposed by Burny et al. (1984). As shown in Fig. 5, the progress of healing in patients treated with intramedullary nailing and bone grafting could be assessed by using the ET method. The ET angle *vs.* time relation in these cases was also expressed by exponential curves. However, the ET angle curve of patient 7 (Fig. 6b) did not show any significant decrease of the angle and there was no correlation between the ET angle and time. From this, the healing process was diagnosed as nonunion. The ET angle of patient 8, treated with plating, showed an extremely slow decrease over time from 9 weeks to 33 weeks, but reduction of the angle was statistically significant until 45 weeks, so the healing process was concluded to be delayed.

Fracture site stiffness was adopted as a parameter for evaluation that was thought to be correlated with strength of bone healing. In various earlier studies of fracture site mechanical properties, stiffness was measured to estimate the strength of the fracture site. However, stiffness is not necessarily correlated with strength. Chehade et al. (1997) investigated this relationship in 24

sheep. The tibia was stabilized with an external fixator and then osteotomy was done. Next, the tibiae were excised at 6, 8 and 10 wk after osteotomy and a 4-point bending test was done. As a result, in the initial stage of healing, stiffness showed a strong correlation with strength ($r = 0.89$), but there was no correlation between them in the remodeling stage. However, as Chehade et al. (1997) stated, because the stiffness of the fracture site is strongly correlated with the strength until remodeling is initiated, it is clinically significant to monitor fracture site stiffness as a substitute for strength to determine the appropriate level of weight bearing so that patients can avoid refracture because of overloading the fracture site during postoperative management. In the remodeling stage, we need to pay special attention to the relationship between stiffness and strength, even if stiffness reached the same value as the intact side.

Fracture healing was evaluated quantitatively by the echo tracking method in patients treated conservatively as well as by internal fixation. All previous methods of assessment could only be applied to patients treated with an external fixator that required the insertion of wires or screw pins, and none of the methods could achieve evaluation in a totally noninvasive manner. The potential problem with evaluating patients treated with internal osteosynthetic devices such as intramedullary nails or plates is that the stiffness at the fracture site is the sum of stiffness for both the healing fracture and the implant. The stiffness of the implant is very high compared with that of the healing fracture because it is made of a metal such as stainless steel or titanium-aluminum-vanadium alloy. Therefore, the combined stiffness at the fracture site is usually very high compared with that in patients receiving conservative treatment by casting. In such patients with internal osteosynthetic devices, comparison of stiffness with the intact side does not have any meaning for evaluation of fracture healing. Therefore, we have to be careful with interpretation of the changes of stiffness over time in such cases. How the implanted material and the configuration of stabilization affect fracture site stiffness should be investigated in the future so that we can assess fracture healing more precisely in patients with internal fixation.

In conclusion, it was demonstrated that the echo tracking method could be clinically applicable to evaluate fracture healing as a versatile, quantitative and noninvasive technique. Further development of this method should be performed so that it can be applied to other anatomical sites by improving accuracy and precision.

Acknowledgements—This work was funded in part by a grant from the Pharmaceutical and Medical Devices Agency of Japan.

REFERENCES

Bourgois R, Burny F. Measurement of the stiffness of fracture callus in vivo. A theoretical study. J Biomech 1972;5:85–91.

Burny F, Donkerwolcke M, Bourgois R, Domb M, Saric O. Twenty years experience in fracture healing measurement with strain gauges. Orthopedics 1984;7(12):1823–1826.

Chehade MJ, Pohl AP, Pearcy MJ, Nawana N. Clinical implications of stiffness and strength changes in fracture healing. J Bone Joint Surg [Br] 1997;79-B:9–12.

Hokanson DE, Mozersky DJ, Sumner DS, Strandness DEJ. A phase-locked echo tracking system for recording arterial diameter changes in vivo. J Appl Physiol 1972;32(5):728–733.

Jernberger A. Measurement of stability of tibial fractures. A mechanical method. Acta Orthop Scand 1970;135(suppl):1–88.

Matsuyama J, Ohnishi I, Sakai R, Suzuki H, Harada A, Bessho M, Matsumoto T, Nakamura K. A new method for measurement of bone deformation by echo tracking. Med Eng Phys 2006;28(6):588–595.

Moorcroft CI, Ogrodnik PJ, Thomas PBM, Wade RH. Mechanical properties of callus in human tibial fractures: A preliminary investigation. Clin Biomech 2001;16:776–782.

Nicholls PJ, Berg E. Acoustic emission properties of callus. Med Biol Eng Comput 1981;19(4):416–418.

Watanabe Y, Minami G, Takeshita H, Fujii T, Takai S, Hirasawa Y. Prediction of mechanical properties of healing fractures using acoustic emission. J Orthop Res 2001;19(4):548–553.

THE JOURNAL OF BIOLOGICAL CHEMISTRY VOL. 283, NO. 36, pp. 24682–24689, September 5, 2008

Krüppel-like Factor 5 Causes Cartilage Degradation through Transactivation of Matrix Metalloproteinase 9*[S]

Received for publication, December 3, 2007, and in revised form, June 23, 2008 Published, JBC Papers in Press, July 10, 2008, DOI 10.1074/jbc.M709857200

Yusuke Shinoda[‡], Naoshi Ogata[§], Akiro Higashikawa[‡], Ichiro Manabe[¶], Takayuki Shindo[¶], Takashi Yamada[‡], Fumitaka Kugimiya[‡], Toshiyuki Ikeda[§], Naohiro Kawamura[‡], Yosuke Kawasaki[‡], Kensuke Tsushima[¶], Norifumi Takeda[¶], Ryozo Nagai[¶], Kazuto Hoshi[‡], Kozo Nakamura[‡], Ung-il Chung[§], and Hiroshi Kawaguchi[‡1]

From [‡]Sensory and Motor System Medicine, [¶]Circulatory Medicine, and [§]Bone and Cartilage Regeneration Medicine, University of Tokyo, Tokyo 113-8655, Japan

Although degradation of cartilage matrix has been suggested to be a rate-limiting step for endochondral ossification during skeletal development, little is known about the transcriptional regulation. This study investigated the involvement of KLF5 (Krüppel-like factor 5), an Sp/KLF family member, in the skeletal development. KLF5 was expressed in chondrocytes and osteoblasts but not in osteoclasts. The heterozygous deficient ($KLF5^{+/-}$) mice exhibited skeletal growth retardation in the perinatal period. Although chondrocyte proliferation and differentiation were normal, cartilage matrix degradation was impaired in $KLF5^{+/-}$ mice, causing delay in replacement of cartilage with bone at the primary ossification center in the embryonic limbs and elongation of hypertrophic chondrocyte layer in the neonatal growth plates. Microarray analyses identified MMP9 (matrix metalloproteinase 9) as a transcriptional target, since it was strongly up-regulated by adenoviral transfection of KLF5 in chondrogenic cell line OUMS27. The KLF5 overexpression caused gelatin degradation by stimulating promoter activity of MMP9 without affecting chondrocyte differentiation or vascular endothelial growth factor expression in the culture of chondrogenic cells; however, in osteoclast precursors, it affected neither MMP9 expression nor osteoclastic differentiation. KLF5 dysfunction by genetic heterodeficiency or RNA interference was confirmed to cause reduction of MMP9 expression in cultured chondrogenic cells. MMP9 expression was decreased in the limbs of $KLF5^{+/-}$ embryos, which was correlated with suppression of matrix degradation, calcification, and vascularization. We conclude that KLF5 causes cartilage matrix degradation through transcriptional induction of MMP9, providing the first evidence that transcriptional regulation of a proteinase contributes to endochondral ossification and skeletal development.

Endochondral ossification is an essential process for skeletal development and growth (1). During the process, chondrocytes undergo proliferation and hypertrophic differentiation. The hypertrophic chondrocytes then secrete a specialized extracellular matrix rich in type X collagen (COL10),[2] which is replaced by bone matrix. The ossification begins with chondrocyte apoptosis, cartilage matrix degradation, calcification, vascular invasion from perichondrium and bone marrow, and deposition of bone matrix by osteoblasts (2). Among these individual steps, previous studies have indicated that degradation of cartilage matrix is particularly crucial (3–6). This step requires proteolytic breakdown by a variety of proteinases, among which members of the matrix metalloproteinase (MMP) family are of special interest due to their ability to cleave collagens and aggrecan, the two principal matrix components of cartilage (7, 8). However, little is known about transcriptional regulation of MMPs in the endochondral ossification process.

Members of the Krüppel-like factor (KLF) family are important transcription factors that regulate development, cellular differentiation and growth, and pathogenesis of atherosclerosis and tumor development, by controlling the expression of a large number of genes with GC/GT-rich promoters (9). There are currently 17 known members of the mammalian KLF family (10), each of which has individually important biological functions (11). Among the members, KLF5 (IKLF, BTEB2) was identified as a positive regulator of SMemb, a marker gene for activated smooth muscle cells in vascular disease (12). KLF5 shows temporal changes in expression during embryogenesis, with diverse functions in cell differentiation and embryonic development (13, 14). Although KLF5 homozygous knock-out ($KLF5^{-/-}$) mice die *in utero* before embryonic day 8.5 (E8.5), the heterozygous knock-out ($KLF5^{+/-}$) mice are apparently normal and fertile (15). Further analyses of these mice revealed that KLF5 mediates cardiovascular remodeling, since the mice exhibited attenuated cardiac hypertrophy and fibrosis as well as much less granulation formation in response to vascular injury (15). The neonatal $KLF5^{+/-}$ mice also exhibited a marked deficiency in white adipose tissue development, suggesting a contribution to adipogenesis (16).

The KLF family shares similar zinc finger structures with the Sp family, some members of which are known to be essential for

* This work was supported by Grants-in-aid for Scientific Research 16659401 and 18209047 from the Japanese Ministry of Education, Culture, Sports, Science, and Technology. The costs of publication of this article were defrayed in part by the payment of page charges. This article must therefore be hereby marked "*advertisement*" in accordance with 18 U.S.C. Section 1734 solely to indicate this fact.

[S] The on-line version of this article (available at http://www.jbc.org) contains supplemental Tables 1 and 2 and Figs. 1–5.

[1] To whom correspondence should be addressed. Tel.: 81-33815-5411 (ext. 30473); Fax: 81-33818-4082; E-mail: kawaguchi-ort@h.u-tokyo.ac.jp.

[2] The abbreviations used are: COL10, type X collagen; COL2, type II collagen; KLF, Krüppel-like factor; M-CSF, macrophage-colony stimulation factor; M-BMMΦ, M-CSF dependent-bone marrow macrophages; MMP, matrix metalloproteinase; TRAP, tartrate-resistant acid phosphate; RANKL, receptor activator of nuclear factor κB ligand; HE, hematoxylin and eosin; TUNEL, terminal dUTP nick-end labeling; EV, empty vector; RT, reverse transcription; VEGFA, vascular endothelial growth factor A; *En*, embryonic day *n*; ADAMTS, a disintegrin and metalloproteinase with thrombospondin-like repeat.

skeletal development and growth. For example, Sp3 and Sp7 (osterix) are required for skeletal ossification (17) and osteoblast differentiation (18), respectively. The present study initially detected KLF5 expression in cells of bone and cartilage. To learn the role of KLF5, we analyzed the skeleton of KLF5$^{+/-}$ mice and found that the KLF5 insufficiency caused impaired degradation of cartilage matrix in the perinatal period. We further investigated the underlying molecular mechanisms.

EXPERIMENTAL PROCEDURES

Mice—Generation of KLF5$^{+/-}$ mice was described previously (15). All mice were maintained in the C57BL/6 background with a standard diet. In each experiment, male mice of KLF5$^{+/-}$ and the wild-type littermates were compared. All experiments were performed according to the protocol approved by the Animal Care and Use Committee of the University of Tokyo.

Cell Cultures—Mouse osteoblastic cell line MC3T3-E1, mouse chondrogenic cell line ATDC5, and mouse monocyte-macrophagic cell line RAW264.7 were purchased from RIKEN. Human chondrogenic cell line OUMS27 was purchased from the Health Science Research Resources Bank. For isolation of primary osteoblasts, calvariae of neonatal wild-type mice were digested for 10 min at 37 °C in an enzyme solution containing 0.1% collagenase and 0.2% dispase five times, and cells isolated by the last four digestions were combined. Primary chondrocytes were prepared from ventral rib cages (excluding the sternum) of E18.5 wild-type mouse embryos as previously described (19). For mature osteoclasts, macrophage colony-stimulating factor (M-CSF)-dependent bone marrow macrophages (M-BMMΦ), which are known to be osteoclast precursors, were isolated from bone marrow of 6–8-week-old mice, as previously described (20), and cultured in the presence of M-CSF (30 ng/ml) and soluble receptor activator of nuclear factor κB ligand (RANKL; 100 ng/ml) for 3 days. Primary osteoblasts and MC3T3-E1 cells were cultured in α-minimal essential medium containing 10% fetal bovine serum. Primary chondrocytes, ATDC5, OUMS27, and Raw264.7 cells were cultured in Dulbecco's modified Eagle's medium containing 10% FBS. For proliferation assay of primary chondrocytes, cell number was counted using Cell Counting Kit-8 (Dojindo).

Histological Analyses—The whole skeletons of wild-type and KLF5$^{+/-}$ littermate embryos (E16.5) were fixed in 99.5% ethanol, transferred to acetone, and stained in a solution containing Alizarin red S and Alcian blue 8GX (Sigma). Tibial limbs were fixed in 4% paraformaldehyde/PBS, embedded in paraffin, sectioned in 5-μm slices, and stained with hematoxylin and eosin (HE), toluidine blue, Safranin-O, and 5% silver nitrate (von Kossa), according to the standard procedures. TUNEL staining was performed using an apoptosis *in situ* detection kit (Wako), according to the manufacturer's instruction. TRAP-positive cells were stained at pH 5.0 in the presence of L-(+)-tartaric acid using naphthol AS-MX phosphate in *N,N*-dimethyl formamide as the substrate. For immunohistochemistry, rabbit anti-mouse antibodies against KLF5 (1:100; KM1785) (15), type II collagen (COL2) (1:1000; LSL), COL10 (1:1000; LSL), and osteopontin (1:1000; LSL), a goat anti-mouse antibody against MMP9 (1:150; R&D), a mouse anti-mouse antibody against the aggrecan DIPEN neoepitope (1:100; ab3777; Abcam), and a rat anti-mouse antibody against CD34 clone MEC14.7 (1:50; Hycult Biotech) were used. For bromodeoxyuridine labeling, animals were injected intraperitoneally with bromodeoxyuridine (25 μg/g body weight; Sigma) 2 h prior to sacrifice, and the sections were stained with a bromodeoxyuridine staining kit (Zymed) according to the manufacturer's instructions.

Viral Transfections and Osteoclastogenesis Assay—For adenovirus infection of KLF5 to OUMS27 cells, the construction of adenovirus KLF5 expression vector was described previously (21). Adenovirus expressing KLF5 or the control empty vector (EV) was transduced to the cells at 40 or 100 multiplicities of infection. At 72 h after transfection, the cells were harvested and used for subsequent assays. For retrovirus infection of KLF5 to M-BMMΦ, the construction of retrovirus KLF5 expression vector was described previously (16). M-BMMΦ were infected with KLF5 or control retroviral particles and further cultured with M-CSF (30 ng/ml) and soluble RANKL (100 ng/ml) for 4–5 additional days, and then the number of cells positively stained for TRAP and containing more than three nuclei were counted as osteoclasts.

RNA Interference—Small interfering RNA oligonucleotides were constructed by DHARMACON. They were transfected to OUMS27 cells in concentrations of 200 nM, according to the manufacturer's instructions, and cultured for 72 h for subsequent assays. Small interfering RNA probe sequences are described in the supplemental materials.

Real Time RT-PCR, Western Blotting, and Gelatin Zymography—For RT-PCR, total RNAs were reverse-transcribed with MultiScribe reverse transcriptase (ABI). Real time PCR was performed on an ABI Prism 7000 sequence detection system (ABI) using QuantiTect SYBR Green PCR Master Mix (Qiagen), according to the manufacturer's instructions. Sequence information is described in the supplemental materials. For Western blot analysis, primary antibody to KLF5 (1:1000; KM1785) (15), MMP9 (1:1000; R&D), or β-actin (1:2000; Sigma) was used. For gelatin zymography, 10 μg of cell lysates was loaded to a zymogram acrylamide gel. The gel was electrophophoresed and incubated with developing buffer for 40 h using a Zymography Electrophoresis kit (Cell Garage).

Microarray Analysis—Target genes of KLF5 were identified by comparing mRNA expression in OUMS27 cells with adenoviral introduction of KLF5 or EV using two systems of microarray analyses: APHS-016 (for human extracellular matrix and adhesion molecules; supplemental Table 1) and APHS-024 (for human angiogenesis molecules; supplemental Table 2) in an RT2 Profiler PCR Array System (Super Array Bioscience). For MMP19 and -20 and ADAMTS4, -5, -9, and -15, which are not included in the array systems, real time RT-PCR analysis was separately performed. Sequence information is described in the supplemental materials.

Luciferase Assay—The human MMP9 promoter regions from −1,250 bp relative to the transcriptional start site were cloned into the pGL4-Basic vector (Promega). The luciferase assay was performed with a dual luciferase reporter assay system (Promega) using GloMax™ 96 Microplate Luminometer (Promega).

Radiological Analyses—Plain radiographs were taken using a soft x-ray apparatus (CMB-2, SOFTEX), and bone mineral density was measured by dual energy x-ray absorptiometry using a bone mineral analyzer (PIXImus, Lunar Corp.).

Bone Fracture Experiment—A transverse osteotomy was created at the midshaft of the right tibia using a bone saw and was internally stabilized with an intramedullary nail using the inner pin of a spinal needle of 22- or 23-gauge diameter depending on the size of the cavity, as we reported previously (22, 23). For histological analyses, specimens of the harvested tibias were fixed with 4% paraformaldehyde, decalcified with EDTA, dehydrated with ethanol, embedded in paraffin, and cut into 5-μm sections. The sections were stained with HE or toluidine blue.

Arthritis Experiment—Arthritis was induced by the modified method of Terato *et al.* (24, 25). Briefly, mice were injected intraperitoneally with 10 mg of an anti-COL2 monoclonal antibody (Immuno-Biological Laboratory) on day 0. On days 2 and 7, 50 μg of lipopolysaccharide (100 μl of 500 μg/ml solution in saline) was injected intraperitoneally, followed by an intermittent lipopolysaccharide injection every 3 days to the end of the experiment. As a control, 2.5 and 0.1 ml of saline was injected similarly to the antibody and lipopolysaccharide, respectively. The clinical severity of arthritis was graded on a 0–3 scale as follows: 0, normal; 1, swelling of ankle or wrist or limited to digits; 2, swelling of the entire paw; 3, maximal swelling. Each limb was graded by a single blinded observer, allowing a maximum arthritis score of 12 for each animal.

Statistical Analysis—Means of groups were compared by analysis of variance, and significance of differences was determined by *post hoc* testing using Bonferroni's method.

RESULTS

KLF5 Expression in Bone and Cartilage—To know the involvement of KLF5 in skeletal metabolism, we initially examined the expression of KLF5 mRNA in cells of bone and cartilage by RT-PCR analysis (Fig. 1*A* and supplemental Fig. 1*A*). It was expressed in primary osteoblasts and chondrocytes derived from mouse neonatal calvaria and costal cartilage, respectively, as well as in osteoblastic cell line MC3T3E1 and chondrogenic cell lines ATDC5 and OUMS27. Meanwhile, the expression was hardly detected in osteoclasts formed from the precursor M-BMMΦ (20) or in monocyte-macrophagic cell line RAW264.7. Immunohistochemical analysis of tibial limbs of mouse embryos and neonates showed extensive expression of KLF5 in cells of all layers of cartilage and perichondrium as well as in osteoblasts on primary spongiosa (Fig. 1*B*). The expression in chondrocytes of limb cartilage was visible as early as E13.5 (supplemental Fig. 1*B*).

Impaired Cartilage Degradation and Remodeling in KLF5$^{+/-}$ Limbs—To learn the physiological function of KLF5 *in vivo*, we investigated the skeletal phenotype of KLF5$^{+/-}$ mice, because KLF5$^{-/-}$ mice died before E8.5 (15). Although KLF5$^{+/-}$ embryos (E16.5) showed normal skeletal patterning without abnormality in major organ development, they were smaller in size compared with wild-type littermates (Figs. 2, *A* and *B*). The femoral and tibial limbs of KLF5$^{+/-}$ embryos were 10–15% shorter than those of the wild-type littermates. In the KLF5$^{+/-}$ limb shaft, formation of bone and bone marrow tissues around

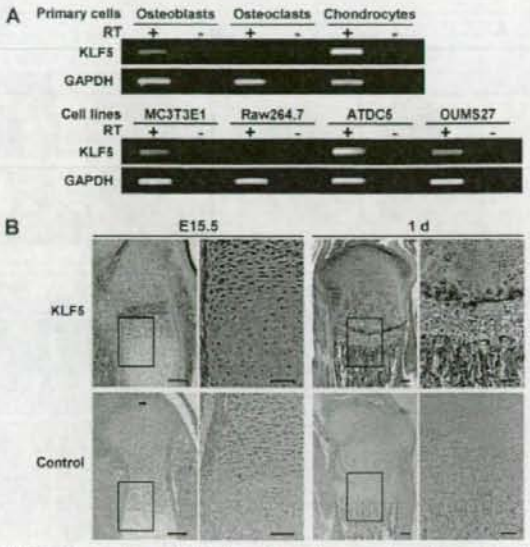

FIGURE 1. **Expression of KLF5 in cells of bone and cartilage.** *A*, mRNA expression of KLF5 and glyceraldehyde 3-phosphate dehydrogenase (*GAPDH*) as the loading control, determined by RT-PCR in mouse primary cells (*upper lanes*) (neonatal calvarial osteoblasts, mature osteoclasts formed from M-BMMΦ with M-CSF and RANKL stimulation, and neonatal costal chondrocytes) and cell lines (*lower lanes*) (osteoblastic cell line MC3T3E1, monocyte-macrophagic cell line Raw264.7, and chondrogenic cell lines ATDC5 and OUMS27). *B*, localization of KLF5 determined by immunohistochemistry by an antibody to KLF5 or the control nonimmune serum in tibial limbs of mouse embryo (E15.5) and neonate (1 day). The *inset boxes* in the *left panels* indicate the regions of the respective *right panels*. *Scale bars*, 100 and 50 μm in *left* and *right panels*, respectively.

the primary ossification center was delayed (Fig. 2*B*), and cartilage matrix like COL2 or COL10 remained undegraded in the shaft (Fig. 2*C*). Accordingly, TUNEL-positive apoptotic chondrocytes and tartrate-resistant acid phosphatase (TRAP)-positive osteoclasts/chondroclasts were decreased in the KLF5$^{+/-}$ limb. In the growth plate of neonates, although there was no difference in proliferative and prehypertrophic layers between the genotypes, the hypertrophic layer was elongated in KLF5$^{+/-}$ mice (Fig. 2, *D* and *E*). The Safranin-O-positive proteoglycan matrix remained in the hypertrophic layer, whereas the von Kossa-positive calcification layer was reduced in the KLF5$^{+/-}$ growth plate. These results indicate that the KLF5 insufficiency causes impairment of cartilage degradation and calcification in the perinatal period.

In an earlier period prior to the occurrence of ossification in the limb shaft of wild-type mice (E15.5), the limbs were filled with chondrocytes with comparable production of proteoglycan, COL10, and osteopontin in KLF5$^{+/-}$ and the wild-type littermates, indicating that KLF5 insufficiency did not affect chondrocyte differentiation in early stages up to hypertrophic differentiation (supplemental Fig. 2*A*). Chondrocyte proliferation determined by bromodeoxyuridine uptake was also similar between the genotypes (supplemental Fig. 2*B*).

After birth, skeletal growth of KLF5$^{+/-}$ mice caught up with that of wild type, and they became comparable at 4 weeks of age (supplemental Fig. 3, *A* and *B*). KLF5 did not affect bone remodeling after birth either, since bone density of KLF5$^{+/-}$ long bones was normal (supplemental Fig. 3, *C* and *D*).

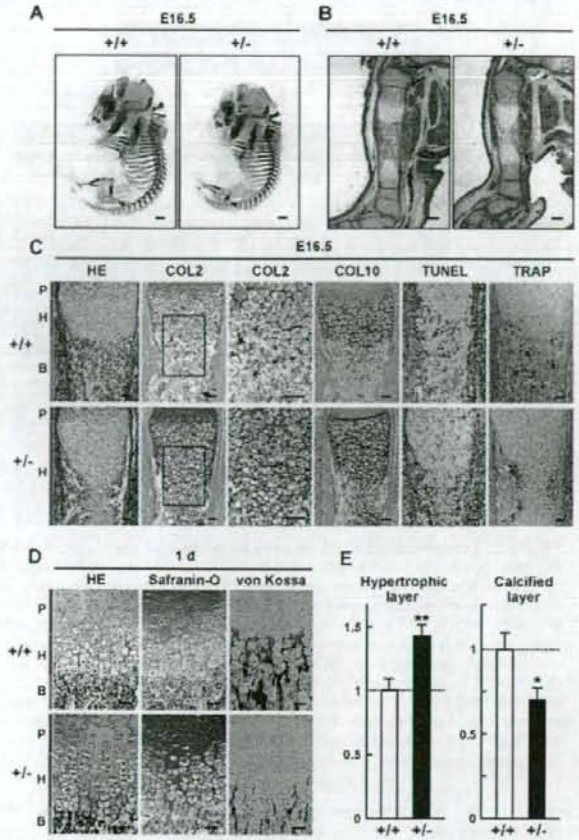

FIGURE 2. **Skeletal phenotypes of KLF5$^{+/-}$ mice in the perinatal period.** *A*, skeletal staining with Alizarin red and Alcian blue; *B*, HE staining of the tibial limbs of wild-type (+/+) and KLF5$^{+/-}$ embryos (E16.5). *Scale bars*, 1 mm and 200 μm, respectively. *C*, HE, COL2, and COL10 immunostainings and TUNEL and TRAP stainings of the tibial limbs of wild-type and KLF5$^{+/-}$ embryos (E16.5). *Inset boxes* in the *left COL2 panels* indicate the regions of the respective *right COL2 panels*. *Blue*, *red*, and *green bars* indicate proliferative (*P*) and hypertrophic (*H*) layers and bone area (*B*), respectively. *Scale bars*, 50 μm. *D*, HE, Safranin-O, and von Kossa stainings of the growth plates in proximal tibias of wild-type and KLF5$^{+/-}$ neonates (1 day). *Scale bars*, 50 μm. *E*, relative lengths of hypertrophic layer (*left*) and calcified layer (*right*) in KLF5$^{+/-}$ growth plate compared with those in wild type (1 day). Data are expressed as means (*bars*) ± S.E. (*error bars*) for 4 mice/group. *, $p < 0.05$; **, $p < 0.01$ *versus* wild type.

MMP9 as a Transcriptional Target of KLF5 in Chondrocytes—To know the molecular mechanism whereby KLF5 contributes to cartilage degradation, we searched for the transcriptional targets by comparing mRNA levels in human chondrogenic cell line OUMS27 adenovirally transfected with KLF5 and the empty vector using microarray and real time RT-PCR analyses (Table 1). Among molecules related to matrix degradation, MMP9 expression was most strongly up-regulated by the KLF5 overexpression.

MMP9 mRNA level was confirmed to be increased in a dose-dependent manner of adenoviral KLF5 overexpression in OUMS27 cells (Fig. 3*A*). In addition, gelatin zymography revealed an increase of gelatin degradation by KLF5, which was compatible with MMP9 activity but not with MMP2 activity, indicating that KLF5 exhibited proteinase activity via the

TABLE 1

Changes in expression of genes related to matrix degradation by KLF5 overexpression

mRNA levels in OUMS27 cells with adenoviral introduction of KLF5 and the control empty vector were compared by RT2 profiler PCR array (APHS-016; SuperArray Bioscience). For MMP19 and -20 and ADAMTS4, -5, -9, and -15, real time RT-PCR was performed using primer sets shown in the supplemental materials. ND, not detected.

Gene symbol	GenBank™ accession number	Increase
		-fold
MMP1	NM_002421	3.1
MMP2	NM_004530	1.6
MMP3	NM_002422	−1.3
MMP7	NM_002423	−1.4
MMP8	NM_002424	2.1
MMP9	NM_004994	2,143.9
MMP10	NM_002425	−1.1
MMP11	NM_005940	−1.8
MMP12	NM_002426	1.4
MMP13	NM_002427	−2.1
MMP14	NM_004995	2.6
MMP15	NM_002428	3.9
MMP16	NM_005941	−1.6
MMP19	NM_002429	1.6
MMP20	NM_004771	ND
ADAMTS1	NM_006988	−2.5
ADAMTS4	NM_005099	46.6
ADAMTS5	NM_007038	−1.4
ADAMTS8	NM_007037	8.4
ADAMTS9	NM_182920	1.1
ADAMTS13	NM_139028	1.6
ADAMTS15	NM_139055	3.1
TIMP1	NM_003254	3.0
TIMP2	NM_003255	3.8
TIMP3	NM_000362	7.7

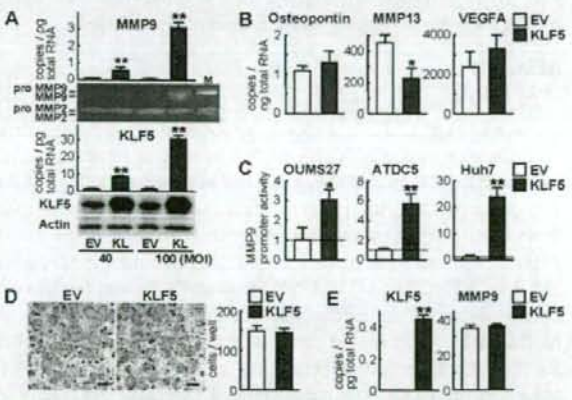

FIGURE 3. **Induction of MMP9 by KLF5 overexpression.** *A*, MMP9 and KLF5 mRNA levels determined by real time RT-PCR analysis after a 3-day culture of human chondrogenic OUMS27 cells adenovirally transfected with empty vector (*EV*) or KLF5 (*KL*) at 40 or 100 multiplicities of infection (*graphs*). Gelatinase activity was determined by gelatin zymography. The *right lane* (*M*) shows markers using recombinant proteins of pro-MMP9, pro-MMP2, and MMP2. KLF5 and actin protein levels were determined by Western blotting. *B*, osteopontin, MMP13, and VEGFA mRNA levels were determined by real time RT-PCR analysis in a 3-day culture of OUMS27 cells adenovirally transfected with 100 multiplicities of infection of EV or KLF5. *C*, MMP9 promoter activity determined by luciferase assay in OUMS27, ATDC5, and Huh7 cells co-transfected with a reporter construct containing the 1,250-bp MMP9 5′-end-flanking region and plasmid vector of EV or KLF5. Data are expressed as relative values compared with EV. *D*, TRAP staining of the osteoclast precursor M-BMMΦ that were retrovirally transfected with EV or KLF5 and cultured with M-CSF and RANKL for 4–5 days. *Scale bars*, 100 μm. The *graph* shows the number of TRAP-positive multinucleated osteoclasts. *E*, mRNA levels of KLF5 and MMP9 determined by real time RT-PCR analysis in the M-BMMΦ cultures. Data are expressed as means (*bars*) ± S.E. (*error bars*). *, $p < 0.05$; **, $p < 0.01$ *versus* EV.

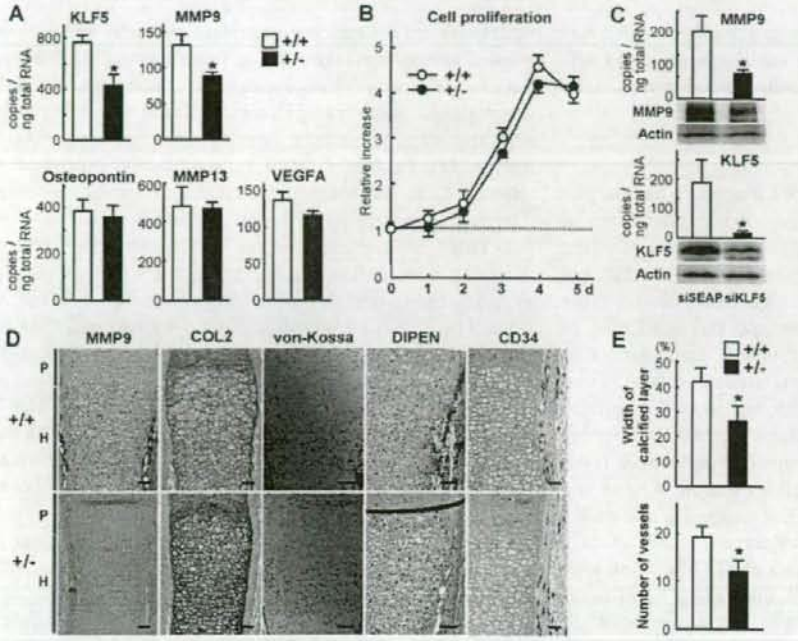

FIGURE 4. **Suppression of MMP9 by KLF5 insufficiency.** *A*, KLF5, MMP9, osteopontin, MMP13, and VEGFA mRNA levels determined by real time RT-PCR analysis in a 3-day culture of primary costal chondrocytes isolated from wild-type (+/+) and KLF5$^{+/-}$ littermates. Data are expressed as means (*bars*) ± S.E. (*error bars*) for 4 mice/group. *, $p < 0.05$ *versus* wild type. *B*, time course of the number of the primary costal chondrocytes above during 5 days of culture. Data are expressed as means (*symbols*) ± S.E. (*error bars*) of the ratios of day 0 for 3 wells/group. *C*, MMP9 and KLF5 mRNA levels determined by real time RT-PCR analysis after a 3-day culture of OUMS27 cells transfected with siSEAP (secreted form of the human placental alkaline phosphatase; control) or siKLF5 oligonucleotides (*graphs*). Data are expressed as means (*bars*) ± S.E. (*error bars*) for 3 wells/group. *, $p < 0.05$ *versus* siSEAP. MMP9, KLF5, and actin protein levels were determined by Western blotting. *D*, MMP9, COL2, DIPEN, and CD34 immunostainings and von Kossa staining of the tibial limbs of E15.5 wild-type and KLF5$^{+/-}$ embryos. *Blue* and *red bars* indicate proliferative (*P*) and hypertrophic (*H*) layers, respectively. *Scale bars*, 50 μm. *E*, the percentage width of the calcified layer to the entire hypertrophic layer determined by the von Kossa staining (*top*) and the number of blood vessels around the hypertrophic layer determined by the CD34 immunostaining (*bottom*) in the growth plates of E15.5 wild-type and KLF5$^{+/-}$ embryos. Data are expressed as means (*bars*) ± S.E. (error bars) for 3 mice/group. *, $p < 0.05$ *versus* wild type.

induction of MMP9. Contrarily, osteopontin mRNA level was not altered by the overexpression, suggesting that chondrocyte differentiation at later stages was not affected by KLF5 (Fig. 3*B*). MMP13 was moderately decreased, whereas vascular endothelial growth factor A (VEGFA) was little regulated by KLF5 in OUMS27 cells, both of which were consistent with the results of microarray analyses (Table 1 and supplemental Tables 1 and 2). To examine the transcriptional regulation, a luciferase reporter gene construct of the MMP9 5′-end-flanking region was transfected into OUMS27, ATDC5, and human hepatocytic Huh7 cells. The transcriptional activity determined by the luciferase reporter assay was enhanced by co-transfection with KLF5 in all cells, demonstrating the transcriptional induction of MMP9 by KLF5 (Fig. 3*C*).

The expression patterns of KLF5 and MMP-9 during chondrocyte differentiation were confirmed to be similar in cultured OUMS-27 cells (supplemental Fig. 1*A*). In addition, the time course analyses by immunostainings of embryonic limbs showed that KLF5 expression was seen early from E13.5, whereas MMP9 expression could be detected at E15.5 and enhanced at E16.5 (supplemental Fig. 1*B*). Since the embryonic stage when the suppression of cartilage degradation in the KLF5$^{+/-}$ limb was initiated around E16.5 (Fig. 2 and supplemental Fig. 2), these time courses support the hypothesis that MMP9 induction by KLF5 may lead to the cartilage degradation during endochondral ossification in skeletal development.

Since MMP9 is known to be strongly expressed in osteoclastic cells (26) and to play an important role in skeletal remodeling (3), we next investigated the effects of KLF5 on the culture of osteoclast precursor M-BMMΦ by retroviral overexpression of KLF5. Neither the osteoclastogenesis nor the MMP9 mRNA level was affected by the overexpression (Fig. 3, *D* and *E*). In the monocyte-macrophagic Raw264.7 cell culture as well, the adenoviral overexpression of KLF5 did not affect endogenous MMP9 mRNA level (supplemental Fig. 4*A*), whereas it increased the activity of the exogenously transfected luciferase reporter construct containing the MMP9 promoter above (supplemental Fig. 4*B*). These findings indicate that KLF5 does not have an important physiological function in osteoclastic cells.

To further examine the effect of loss of function of KLF5 in chondrocytes, we cultured primary costal chondrocytes derived from KLF5$^{+/-}$ mice and confirmed that the KLF5 mRNA level was decreased to about half that of wild-type chondrocytes (Fig. 4*A*). Among the molecules related to terminal differentiation of chondrocytes, cartilage degradation, and remodeling, only MMP9, and not osteopontin, MMP13, or VEGFA, was significantly suppressed by the KLF5 haploinsufficiency. Proliferative ability was comparable between cultured chondrocytes from KLF5$^{+/-}$ and the wild-type littermates (Fig. 4*B*). Gene silencing of KLF5 by RNA interference also caused the reduction of MMP9 mRNA expression in OUMS27 cells (Fig. 4*C*).

Finally, an immunohistochemical staining confirmed that MMP9 expression seen in the cartilage layer and the perichondrium of wild-type limb was scarcely detected in KLF5$^{+/-}$ (Fig. 4*D*). In the cartilage layer, the decreased MMP9 expression was correlated with the suppression of COL2 degradation and chondrocyte calcification, determined by immunohistochemical and von Kossa stainings, respectively. In the perichondrium, the MMP decrease was correlated with the suppression of DIPEN, which is a neoepitope at the aggrecan cleavage site generated by MMPs, and with that of CD34, which is an endothelial antigen representing blood vessels, determined by respective

immunostainings. Quantitative analyses actually revealed significant decreases in the width of the von Kossa-positive calcified layer and the number of CD34-positive blood vessels in the KLF5$^{+/-}$ limb (Fig. 4*E*).

DISCUSSION

The present *in vivo* analyses revealed that KLF5 haploinsufficiency caused impairment of cartilage matrix degradation and the subsequent remodeling to bone tissue, without affecting chondrocyte proliferation or differentiation. Microarray and cell culture analyses demonstrated that KLF5 contributes to the cartilage degradation through transcriptional induction of MMP9. MMP9 is known to be a potent proteinase that degrades denatured collagens and activates other MMPs and cytokines (4, 8, 27). In fact, the homozygous deficient mice (MMP9$^{-/-}$ mice) are reported to exhibit skeletal abnormality similar to KLF5$^{+/-}$ mice: elongation of hypertrophic layer, impaired vascularization, and delayed formation of bone and bone marrow cavity in the limbs (3), indicating a role of the KLF5-MMP9 axis during skeletal development.

It is, however, of note that the defect of KLF5 is physiologically more critical than that of MMP9, since KLF5$^{-/-}$ mice die *in utero* before E8.5, whereas MMP9$^{-/-}$ mice grow normally after birth, and MMP9$^{+/-}$ mice show no abnormality from embryos (3). This might be because KLF5 regulates molecules other than MMP9, since the present microarray analyses revealed up-regulation of several molecules like α-E-catenin (CTNNA1), ADAMTS4 (a disintegrin and metalloproteinase with thrombospondin-like repeat 4), interleukin-1, and MMP14 by the KLF5 overexpression in chondrogenic cells (Table 1 and supplemental Tables 1 and 2). α-E-catenin, a prototypic member of the α-catenin family and a component of the cadherin-catenin complex (28), is known to be required to sustain adhesion between cells during mammalian morphogenetic events (29). Although it is mainly expressed in epithelial tissues and the loss-of-function mutation causes human squamous cell carcinoma of the skin (30), the involvement in matrix degradation or angiogenesis remains unknown. Meanwhile, ADAMTS4 is a principal proteinase for aggrecan (31), a major cartilage matrix component that is degraded before collagenases cleave collagens in the hypertrophic layer (32). Hence, KLF5 might possibly lead to aggrecan degradation through induction of ADAMTS4, which is followed by matrix degradation by MMP9 (5). Interleukin-1, a representative proinflammatory cytokine, is also known to be a potent stimulator of MMPs, ADAMTSs, and other catabolic cytokines (32), so that interleukin-1 and MMP9 induced by KLF5 might initiate the subsequent catabolic changes of the cartilage. MMP14, although the induction by KLF5 was not strong (Table 1), is also a key proteinase in growth plate resorption, since the MMP-14-deficient mice exhibited dwarfism due to impaired endochondral ossification and angiogenesis, similarly to the KLF5$^{-/-}$ mice (33, 34). KLF5 may therefore be a crucial transcription factor that controls the molecular network for cartilage matrix degradation during endochondral ossification.

Another difference in the effects of insufficiency of KLF5 and MMP9 is their function in osteoclasts or chondroclasts. MMP9$^{-/-}$ mice showed abnormal bone remodeling after birth with impaired osteoclast recruitment, whereas KLF5$^{+/-}$ mice showed normal bone remodeling. Expression of MMP9 by osteoclastic cells may physiologically be important for skeletal development, since transplantation of wild-type bone marrow cells, including osteoclast progenitors, rescues the skeletal phenotype (3). In fact, MMP9 is abundantly expressed (26), whereas KLF5 was barely detected in osteoclastic cells (Fig. 1). The finding that the KLF5 overexpression in osteoclast precursors failed to alter endogenous MMP9 expression and osteoclastic differentiation (Fig. 3, *D* and *E*, and supplemental Fig. 4) supports the importance of MMP9 expression in osteoclastic cells. The present study, however, demonstrated that other than in osteoclasts, MMP9 was expressed in chondrocytes and perichondrium during skeletal development and was dramatically decreased by the KLF5 haploinsufficiency (Fig. 4*D*). This decrease was correlated with the suppression of COL2 degradation and an aggrecan cleavage neoepitope DIPEN. In addition, the induced MMP9 in chondrocytes by the KLF5 overexpression exerted a potent enzyme activity by gelatin zymography (Fig. 3*A*), as previously reported (35). These indicate a significant role of cell-autonomous action of MMP9 in chondrocytes in the process of cartilage degradation.

For endochondral ossification of hypertrophic chondrocytes, chondrocyte apoptosis, cartilage matrix degradation, and vascularization are tightly coupled (2, 5); however, which of these steps is rate-limiting remains unclear. A recent study on knockout mice of an antiapoptotic protein, galectin 3, has shown that acceleration of chondrocyte apoptosis was not associated with endochondral ossification (36), suggesting that chondrocyte apoptosis might be dispensable for the process. Several reports have indicated the matrix degradation and vascularization as the crucial steps (3, 5, 37–39), and, in fact, the present *in vivo* analyses showed that suppressions of MMP9 expression and cartilage matrix degradation by KLF5 insufficiency led to impairment of skeletal development accompanied by decreased vascularization (Fig. 4*D*). *In vitro* cultures, however, showed that a principal angiogenic factor, VEGFA (37–40), was little influenced by gain or loss of function of KLF5 in chondrocytes (Figs. 3*B* and 4*A*); nor were other angiogenic factors, VEGFC, VEGFD (41), HGF (42), FGF1, or FGF2 (43, 44), in the microarray analyses (supplemental Table 2). Hence, KLF5 is likely to regulate vascularization indirectly as a secondary effect of MMP9 secretion and matrix degradation in the cartilage layer and perichondrium, although the details need to be further investigated. In fact, cartilage explants from MMP9$^{-/-}$ mice in culture are reported to show a delayed angiogenesis (3). A previous report on MMP13$^{-/-}$ and MMP9$^{-/-}$ mice also showed that the cartilage matrix degradation was decreased in parallel with the pace that vasculature recruitment maintains with the slower rate of endochondral ossification (5). This evidence suggests that the matrix degradation may create a permissive environment for blood vessels to invade or make angiogenic factors accessible, leading to a hypothesis that cartilage degradation is a rate-limiting step for endochondral ossification of hypertrophic chondrocytes.

The skeletal abnormality of KLF5+/− mice was limited to the perinatal period and disappeared as the animals grew up after birth under physiological conditions. This may be due